JOURNAL OF MATERIALS SCIENCE 24 (1989) 1117–1120

Tensile and fatigue properties of Fe–Mn–Al–C alloys

S. C. CHANG, Y. H. HSIAU
Department of Materials Science and Engineering, National Tsinghua University, Hsinchu, Taiwan

M. T. JAHN
Department of Mechanical Engineering, California State University, Long Beach, California 90840, USA

The tensile properties and fatigue behaviour of three solution-treated Fe–29 Mn–9 Al–C (wt%) alloys having various carbon contents leading to different volume fractions of austenite and ferrite phases were investigated. The carbon contents were 1.06%, 0.60% and 0.26%, respectively and the corresponding volume fractions of austenite were 100%, 90% and 45%, respectively. The alloy having 1.06% carbon possessed the best tensile properties but its fatigue behaviour was only comparable to the other two alloys with lower carbon contents. The alloy having 0.60% carbon possessed the lowest yield strength, but its fatigue life was slightly better than other two alloys. The alloy having 0.26% C possessed lowest elongation and medium strength, and its fatigue life was comparable to the other two alloys. Their tensile properties and fatigue behaviour were explained in terms of crack initiation, crack propagation, grain size, constituent arrangement and constituent fraction.

1. Introduction

Application of stainless steels, AISI 300 series, has been widely accepted in industry owing to their excellent combination of strength, ductility, toughness and corrosion resistance. However, the alloying elements, nickel and chromium, contained in conventional stainless steels are strategically important and very expensive. In order to ensure adequate supply of stainless steels in the future many studies [1–10] have been done to explore the possibility of the substitution of manganese and aluminium for nickel and chromium. Because the resources of manganese and aluminium are abundant and uniformly distributed on Earth and the prices are much lower than nickel and chromium, the studies of Fe–Mn–Al (Femnal) alloys are exciting and very significant in the development of a new series of stainless steels. In industrial applications, in particular the making of structural and machinery components, the mechanical properties of the alloys are most demanding. Banerji [8] reported that the FeMnAlC system possesses yield and tensile strengths about 50% higher than the conventional stainless steels (300 series) with equivalent ductility. Our recent study [9] shows that at an elongation of 40%, the tensile strength of FeMnAlC alloys can easily reach 150×10^3 p.s.i. ($\sim 1034\,N\,mm^{-2}$) which is roughly twice the tensile strength of the 300 series stainless steels if proper ageing is applied. The study by Charles *et al.* [10] demonstrated that the FeMnAl system is ideal for cryogenic applications such as liquid gas pipelines. As more than 90% of the premature failure of dynamic machinery components is due to fatigue, it is critical that the fatigue behaviour and fatigue mechanisms of Femnal alloys be examined and understood. Unfortunately, little research [11] has been carried out to study the fatigue behaviour of these alloys. The fatigue data obtained [11] were limited to solution-treated, two-phase (austenite and ferrite) FeMnAl alloy with no carbon content. In order to obtain better understanding of the fatigue properties of Fe–Mn–Al–C alloys with different constituent percentages, the fatigue crack initiation, crack propagation and fatigue life of various Fe–Mn–Al–C alloys with different carbon contents were investigated in this study.

2. Materials and methods

Three Femnal alloys with different carbon contents were examined in this work. As shown in Table I the chemical compositions were approximately Fe–29 Mn–9 Al (wt%) and carbon contents ranged from 0.26% to 1.06%. The alloys were prepared by melting appropriate percentages of commercial pure iron, electrolytic manganese, carbon powder and pure aluminium in an induction furnace protected in an argon atmosphere. The ingots were hot forged, homogenized and cold rolled to a thickness of 2 mm. After cold rolling, the plates were solution treated at 1050° C for 1.5 h followed by oil quenching and

TABLE I Chemical compositions (wt%) of specimens A, B and C

	Al	Mn	C	Fe
Alloy A	9.350	28.908	1.063	bal.
Alloy B	9.078	29.187	0.603	bal.
Alloy C	9.160	28.589	0.263	bal.

0022–2461/89 $03.00 + .12

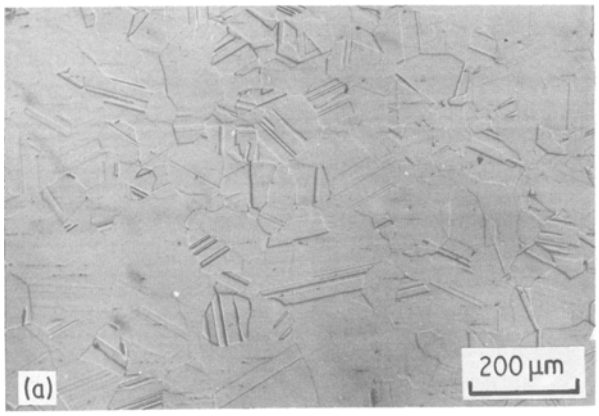

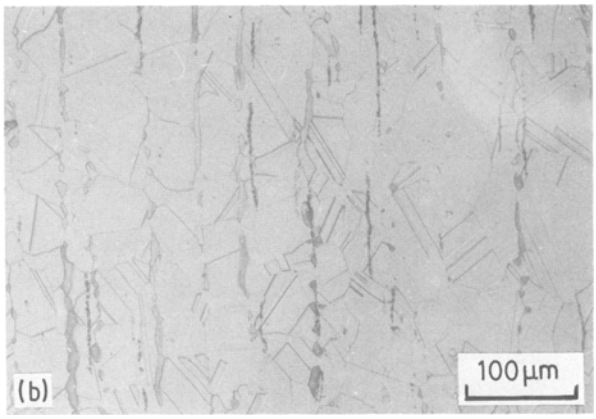

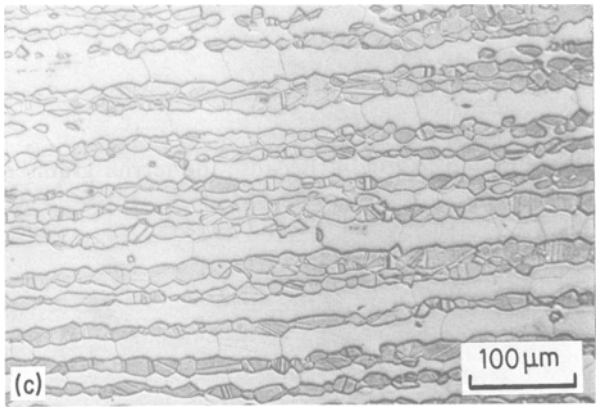

Figure 1 Optical microstructure of (a) specimen A, (b) specimen B and (c) specimen C.

specimen machining. Specimens A, B and C have carbon contents of 1.06%, 0.6% and 0.26%, respectively. The microstructure, fatigue crack initiation and crack propagation were investigated using an optical microscope. The fatigue fracture surfaces were examined using a scanning electron microscope operated at 22 kV. Tensile testing was conducted with an Instron testing machine model 1115 at room temperature. The stress direction was parallel to the rolling direction of specimen. The cross-head speed was 0.182 cm min^{-1}. Fatigue testing was carried out at room temperature with a Sonntag model SF2U reverse banding fatigue machine, the frequency was 1800 c.p.m. The fatigue stress direction was along the rolling direction of specimen. Before fatigue testing, the specimens were wet ground and mechanically polished up to 1200 grit number followed by electrolytic polishing in a solution of 10% perchloric acid and 90% acetic acid.

3. Experimental results and discussion

The microstructures of specimens A, B and C are shown in Figs 1a, b and c, respectively. Specimen A possessed full austenite structure owing to its high carbon and high manganese contents. It is well established that carbon and manganese are austenite formers in steel. Specimens B and C were dual phase (austenite and ferrite) because of lower carbon contents. Specimen B contained 10% ferrite and 90% austenite. Specimen C consisted of 55% ferrite and 45% austenite. The austenite grain size in specimen A was the largest (roughly 100 μm) and the austenite grain size in specimen C was the smallest (roughly 30 μm). The austenite grain size in specimen B was about 60 μm. The ferrite grain sizes in specimens B and C were 10 and 40 μm, respectively. It was also observed that in specimens B and C bunches of ferrite and austenite grains were connected to the same type of grain along the rolling direction.

The tensile test results are summarized in Table II. Specimen A possessed the highest ultimate tensile strength (UTS = 888.1 MPa), highest yield strength (Ys = 551.6) and the largest elongation (El = 59%) compared to specimens B and C. The high strengths can be attributed to the high carbon content (about 1.0%) in specimen A which demonstrates significant solid solution strengthening of austenite phase. The best elongation of specimen A is due to its full austenite phase because austenite steel in general possesses better ductility than ferrite steel. Specimen A is a very tough alloy steel because of its high strength and high ductility. The UTS of specimens B and C were almost equal (about 785 MPa) even though the carbon content of specimen B is significantly higher than specimen C. In addition, specimen B, possessing a higher carbon content, had a much lower yield strength (390 MPa) than that of specimen C (472 MPa). These surprising results can be explained by two mechanisms. Firstly, in specimen B the ferrite volume fraction was very low (10%), and the ferrite grain size was very small (10 μm) as compared to its austenite grain size (60 μm). During tensile testing, the strain incompatibility along the boundaries of ferrite and austenite grains may induce stress concentration inside the ferrite grain. The stress concentration will enhance the multiplication and slip of dislocations such that the yield strength and tensile strength are lowered. Secondly, it is possible that some strengthening alloying elements inside the ferrite phase may diffuse to the grain boundary during heat treatment such that the ferrite grain is weakened. In specimen B the ferrite grain size was much smaller than the ferrite grain size of specimen C. This means that the alloying element diffusion path in specimen B was much shorter than specimen C, therefore, the alloying elements in

TABLE II Tensile properties of specimens A, B and C

Alloy	UTS (MPa)	0.2% YS (MPa)	El (%)
A	888.1	551.6	59.0
B	786.0	390.0	51.0
C	784.0	471.8	35.3

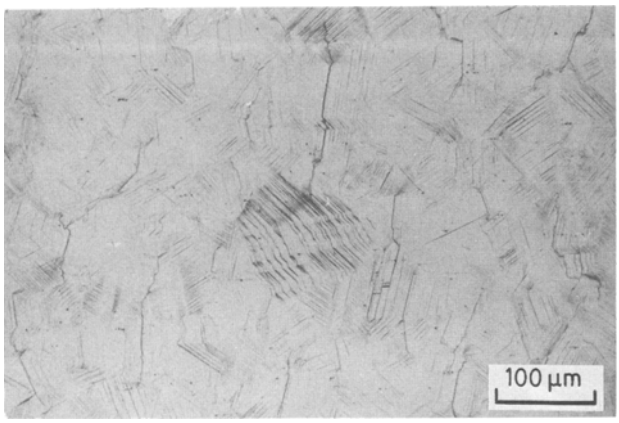

Figure 2 Fatigue cracks and persistent slip bands on the free surface of specimen A.

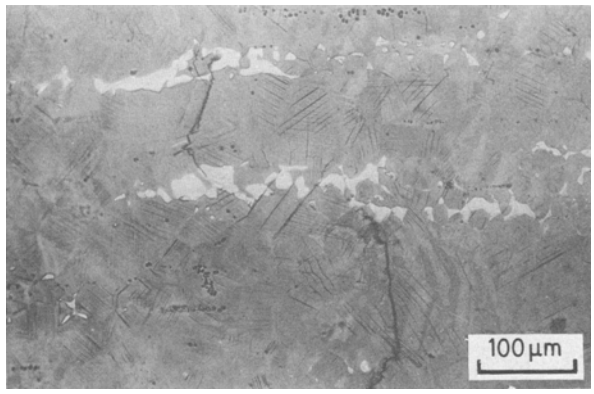

Figure 4 Some fatigue cracks were impeded by ferrite phase of specimen B.

the ferrite grain of specimen B may diffuse to the grain boundary more readily, such that the ferrite grain in specimen B is weakened more significantly. The string arrangement of fine ferrite grains embedded inside the austenite matrix is undesirable not only in strengths but also in corrosion resistance, as reported by two of the authors [12]. The elongation of specimen B was 51%, which is much better than the elongation of specimen C (35.3%). The scanning electron fractographs of specimens A, B and C all showed ductile transgranular fracture with clear and sharp dimples in the over-loaded fractured region and with clear fatigue striations in the fatigue-fractured region. These results are as expected, because the elongation of specimens A, B and C were all very good, above 35%.

It was found that the characteristics of fatigue crack initiation and crack propagation were somewhat different in specimens A, B and C. In specimen A, under cyclic stress, persistent slip bands were generated all over the specimen, the higher the applied stress the higher the density of slip bands. The fatigue cracks mostly initiated and propagated along the persistent slip bands as shown in Fig. 2. The over-all direction of fatigue crack propagation was perpendicular to the stress direction. In specimen B, slip bands apppeared in the austenite phase after fatigue, as shown in Fig. 3. No slip band was found inside the ferrite phase. Mostly, the fatigue cracks also initiated and propagated along the persistent slip bands. It was observed that the ferrite phase in specimen B had the tendency to impede the fatigue crack propagation, as demonstrated in Fig. 4. Because the ferrite grains in specimen B were fine and soft, the blunting effect and intense work hardening during fatigue may explain its impediment to fatigue crack propagation. In specimen C slip bands appeared in both austenite and ferrite phase after cyclic stress. The slip bands in austenite were straight, clear and dense. However, the slip bands in ferrite were ambiguous, wavy and sparse as shown in Fig. 5. Although the slip bands in austenite were denser and sharper than those in ferrite, however, the fatigue cracks mostly initiated along the slip bands in the ferrite phase. As the fatigue cracks grew, they penetrated the austenite region. Our results on the fatigue crack initiation of specimen C are contradictory to Tarn *et al.*s report [11]. Tarn *et al.* [11] observed that in Fe–33 Mn–8 Al alloy with dual phase structure (55% ferrite and 45% austenite) the initiation of fatigue crack was mostly generated within austenite phase, and the ferrite phase possessed higher resistance to fatigue crack initiation and propagation. It is suggested that the difference between our results and Tarn's work is attributed to the different carbon content in Fe–Mn–Al alloys. The volume fraction of the constituents in Tarn *et al.*s alloy is equal to ours. However, Tarn *et al.*s alloy contained 0% carbon whereas our specimen C contained 0.263% carbon.

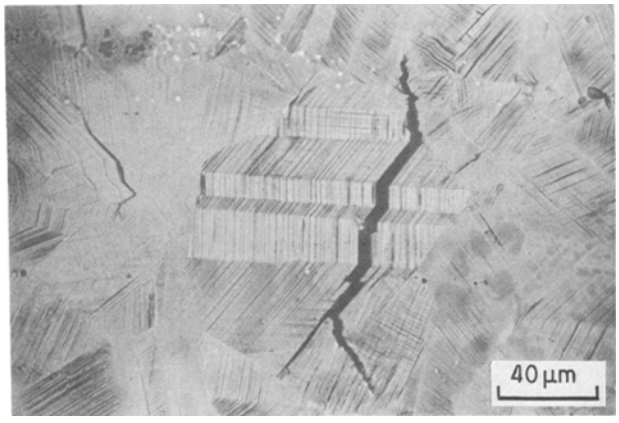

Figure 3 Fatigue cracks and persistent slip bands on the free surface of specimen B.

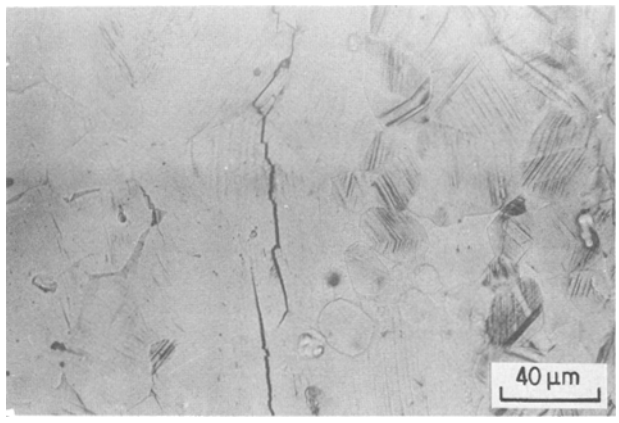

Figure 5 Optical micrograph showing wavy, ambiguous slip bands in ferrite phase and sharp, clear slip bands in austenite phase. Fatigue cracks initiate at slip bands of ferrite phase.

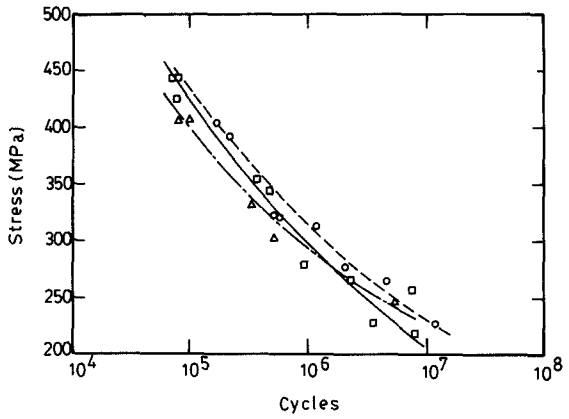

Figure 6 The *S–N* curves of specimens (□, ——) A, (○, – – –) B, (△, – – –) C in reverse bending fatigue test.

The 0.263% carbon was mostly dissolved in the austenite phase such that the austenite phase in specimen C was solid-solution strengthened. Therefore, the fatigue crack would initiate inside the ferrite phase of specimen C instead of inside the solid-solution strengthened austenite phase.

The fatigue life of specimens A, B and C with respect to cyclic stress amplitude is shown in Fig. 6. There is only a slight difference between the *SN* curves of specimens A, B and C. Taking into account the statistical nature of fatigue data, we may consider that specimens A, B and C possessed roughly equal fatigue lives under equal stress amplitude. There are various factors affecting the fatigue life of different specimens. The net results lead to equal fatigue life under equal stress amplitude. For specimen A, the higher carbon content (1.0%) should lead to a higher fatigue life. However, the large grain size (100 μm) and the easy generation of slip bands may offset the beneficial effect of high carbon content. For specimen B, the low yield strength may have a detrimental effect on its fatigue life. However, the small α grains which work as fatigue crack arresters will compensate the detrimental effect of low yield strength. For specimen C, its low carbon content (0.26%) may lead to lower fatigue life. However, the small grain size of the austenite phase and ferrite phase (30 and 40 μm) certainly has a beneficial effect on the fatigue life.

4. Conclusions

The tensile properties and fatigue behaviour of three FeMnAl alloys having various carbon contents leading to different volume fractions of austenite and ferrite phase were investigated. It was found that the grain size, the carbon content and the constituent arrangement are important factors affecting the tensile properties and fatigue behaviour. The fatigue investigation included fatigue crack initiation, fatigue crack propagation and fatigue life. The results can be summarized as follows.

1. Specimen A with highest carbon content (about 1%) and 100% austenite phase possessed the best tensile properties. Its highest strengths (UTS and YS) are attributed to the highest carbon content and the best elongation is due to its 100% austenite.

2. Specimen B with medium carbon content (0.6%) and 90% austenite plus 10% ferrite possessed the lowest yield strength owing to its very fine grain size of soft ferrite embedded in the rather larger grain size of hard austenite. The differences in grain size and hardness may induce strain incompatibility in the vicinity of the ferrite/austenite boundary such that stress concentration occurred inside the ferrite grains during cyclic stress. The strain incompatibility and stress concentration result in the low yield strength of specimen B.

3. In specimens A and B fatigue cracks initiated along the slip bands of the austenite phase. Because the small ferrite grains of specimen B work as fatigue crack arresters, the fatigue life of specimen B was at least as good as specimen A even though the strengths and carbon content of specimen B are much less than specimen A.

4. If the Femnal alloys consist of roughly equal volume fractions of ferrite and austenite phase the fatigue crack may initiate either inside the ferrite grain or the austenite grain depending on the carbon content of the alloy. If the alloy contains almost no carbon the cracks mostly initiate inside the austenite phase [11]. If the alloy contains enough carbon to solid solution strengthen the austentile phase, the fatigue crack will mostly initiate along the slip bands in the ferrite phase, as observed in this investigation.

5. Even though the carbon content of specimen C was the lowest compared to specimens A and B, the fatigue life of specimen C was comparable to specimens A and B because specimen C contains fine ferrite grains and fine austenite grains.

References

1. R. OSHIMA and C. M. WAYMAN, *Met. Trans.* **3** (1972) 2163.
2. T. TADAKI and K. SHIMIZU, *Trans. J. Inst. Metals* **16** (1975) 105.
3. A. INOUE, Y. KOJIMA, T. MINEMURA and T. MASUMOTO, *Met. Trans.* **12A** (1981) 1245.
4. K. H. HAN and W. K. CHOO, *ibid.* **14A** (1983) 973.
5. R. WANG and F. H. BECK, *Metal Progr.* March (1983) 72.
6. P. R. S. JACKSON and G. R. WALLWORK, *Oxid. Metals* **21** (3/4) (1984) 135.
7. T. F. LIU and C. M. WAN, *Scripta Metall.* **19** (1985) 805.
8. S. K. BANERJI, *Metal Progr.* April (1978) 59.
9. S. C. CHANG, M. T. JAHN, Y. C. PAN and C. M. WAN, Proceedings 7th International Conference, Strength of Metals and Alloys, Montreal, Canada, edited by J. McQueen, J. P. Bailon, J. L. Dickson, J. J. Jonas and M. G. Akdan (Pergamon, New York, 1985) p. 429.
10. J. CHARLES, A. BERGHEZAN, A. LUTTS and P. L. DANCOISNE, *Metal Progr.* May (1981) 71.
11. C. L. TARN, C. T. HU and C. M. WAN, *Chinese J. Mater. Sci.* **15** (2) (1983) 75.
12. M. T. JAHN, J. J. CHAN, C. H. KAO, C. M. WAN and S. C. CHANG, Proceedings of Alternate Alloying for Environmental Resistance, TMS-AIME Meeting, New Orleans, March 1986, edited by G. R. Smolik and S. K. Banerji (TMS-AIME, Warrendale, Pennsylvania) p. 179.

Received 23 July
and accepted 23 October 1987